

ACCURACY AND EFFICIENCY OF TRANSITION–TURBULENCE MODELS IN PREDICTING HIGH AND LOW REYNOLDS NUMBER PROPELLER PERFORMANCE

Fernando Parra[1], Diego Domínguez[1], Adrián Delgado[1] & Jesús Gonzalo[1]

[1]Aerospace Engineering Department, I4 Institute, Universidad de León, 24071 León, Spain

Abstract

The emergence of new aerospace vehicles concepts has renewed interest in optimizing propeller design. Among them, several share in common that their propellers operate at low Reynolds numbers. This research assesses the accuracy and efficiency of different transition-turbulence models to determine the convenience of using a more complex turbulence model in computational fluid dynamics. The prediction of propeller performance parameters for both high and low Reynolds propellers are compared using different turbulence models. At high Reynolds number operating conditions, transition-turbulence models provide no advantage, whereas at low Reynolds numbers, $\gamma - Re_\theta$ SST model is preferred. Additionally, at moderate Reynolds number operating conditions γ SST model represents the best compromise between accuracy and computational efficiency. These findings provide insights for selecting turbulence models in propeller aerodynamic design and may help to reduce its computational cost.

Keywords: Propeller aerodynamics, laminar-turbulent transition, laminar separation bubble, turbulence modeling

1. Introduction

The emergence of new aerospace vehicles concepts has renewed interest in optimizing propeller design for aerospace propulsion. These concepts include unmanned stratospheric vehicles, commonly known as High-Altitude Pseudosatellites (HAPS), aircraft relying on Distributed Electric Propulsion (DEP) systems —both employing configurations with multiple propellers or fans distributed along the wing or fuselage as well as eVTOL aircraft— or vehicles developed for space exploration. This trend is further reinforced by the growing demand for commercial aircraft capable of meeting increasingly stringent energy-efficiency, environmental, and operational requirements. The majority of these platforms share in common that, due to small chord lengths, freestream velocities or densities, their propellers operate at low Reynolds numbers.

Low Reynolds number flows are characterized by the increasing importance of viscous forces within the fluid compared to inertial forces [1], the most prominent feature of such flows being the appearance of laminar separation bubbles (LSB) [2], which leads to a nonlinear variation of lift with angle of attack [3]. Consequently, the lower the Reynolds number, the lower the aerodynamic efficiency of airfoils.

As a result, high-fidelity methods must be employed during the design phase, not only to evaluate the aerodynamic performance of the propellers, but also to accurately predict the formation of LSB and minimize their impact on the design. Therefore, the main objective of this study is to analyze the behavior of different transition turbulence models in predicting propeller performance parameters, which are usually influenced by the formation of LSBs at low Reynolds numbers.

2. Transition-turbulence models

The prediction of transition using RANS models is by nature ambiguous [2], as all spectral effects are lost in the time-averaging process employed by turbulence models. Hence, these models cannot reliably determine whether a given perturbation will actually trigger the transition [4], and any predicted transitional behaviour should not be expected to accurately match real physical transition processes. This limitation becomes particularly significant at low Reynolds numbers, where turbulence models are used outside of their intended range of applicability due to the presence of extended laminar or transitional regions. As a result, the use of a turbulence model coupled with a transition model is more appropriate [5].

Existing transition-turbulence models can be classified into three categories [2]: (i) models that use damping functions to limit turbulence production in the viscous sublayer, commonly referred to as *low-Reynolds* models, (ii) models that rely on empirical correlations and (iii) models that attempt to model the transition-related phenomena within a more theoretical framework.

To this end, this analysis considers several transition-turbulence models representative of the categories defined above. First, Menter's $k-\omega$ Shear Stress Transport (SST) model —with Wilcox's low Reynolds modification— is selected as representative of the first category. Second, the empirical correlation based Langtry's $\gamma - Re_\theta$ model and its simplified version, the Menter and Langtry's γ model, are analyzed. Finally, the physics-based Walter and Cockljat's $k - k_l - \omega$ model is employed.

In the following, a brief description of how the different transition-turbulence models attempt to model transitional phenomena is presented.

2.1 $k-\omega$ SST *low-Re* turbulence model

This version of the standard $k-\omega$ Shear Stress Transport (SST) turbulence model, originally developed by Wilcox [4], employs an artificial damping on the closure terms and on the definition of turbulent viscosity [2].

Initially, the boundary layer remains laminar, and the turbulence energy k is entrained from the free-stream and spreads throughout the boundary layer. At a critical Reynolds number, where production of turbulent kinetic energy exceeds its dissipation ω, the transition point is reached and eddy viscosity increases rapidly. Turbulent kinetic energy continues to be amplified until production catches dissipation in ω equation. Now, ω is amplified and continues to grow until a balance between production and dissipation of k is achieved, indicating a fully turbulent flow [4].

However, a number of deficiencies —independent of flow conditions— directly related to the damping functions have been identified in [2]: (i) the model predicts natural transition too early, (ii) it is not able to properly predict separation-induced transition, (iii) the prediction of transition can be coincidental and (iv) it is not able to capture factors that affect transition, such as the adverse pressure gradient or turbulence intensity.

2.2 $\gamma - Re_\theta$ transition-turbulence model

This model, developed by Menter and Langtry [6, 7], aims to overcome the difficulties of *low-Reynolds* turbulence models in accurately predicting transition. To this end, two additional transport equations are coupled with those of the $k-\omega$ SST turbulence model.

An intermittency equation is used to to trigger the transition process by activating the production term of the turbulent kinetic energy downstream of the transition point, whereas a second equation —formulated in terms of the transition onset momentum-thickness Reynolds number, $\tilde{Re}_{\theta t}$— is employed to capture the nonlocal influence of the turbulence intensity. It should be noted that these transport equations do not attempt to model the physics of the transition process, which is contained entirely in the experimental correlations provided to the model [6].

The transition onset Reynolds number is established in the free-stream through experimental correlations, and it is diffused into the boundary layer. When a certain critical momentum-thickness Reynolds number, $Re_{\theta c} = f\left(\tilde{Re}_{\theta t}\right)$, is achieved, the production of intermittency is triggered, which initiates the production of turbulent kinetic energy, leading to transition [2].

2.3 γ transition-turbulence model

This transition-turbulence model is a simplified formulation of the $\gamma - Re_\theta$ model [8], which is built upon the downsides found in it [2] regarding the today's requirements for transition-turbulence models, as resumed in [9]. The γ model avoids the transport equation for the momentum-thickness Reynolds number by evaluating the correlations inside the boundary layer and not outside. Like the $\gamma - Re_\theta$ model, it employs transition onset criteria in terms of Re_θ, but computes the latter algebraically using local variables [8]. As in the $\gamma - Re_\theta$ model, the γ model is coupled with the $k - \omega$ SST turbulence model [10].

2.4 $k - k_l - \omega$ transition-turbulence model

The $k - k_l - \omega$ transition-turbulence model is a three equation physics-based model proposed by Walters and Cokljat [11]. It uses a model equation for the laminar fluctuation energy that is then linked to the underlying $k - \omega$ turbulence model through source and sink terms. By this mechanism, the laminar kinetic energy can be transferred into the turbulent kinetic energy equation and initiate the transitional process. It uses several threshold functions to trigger the transition onset, which are similar in nature to those used in the $\gamma - Re_\theta$ model [8].
The main advantage of the $k - k_l - \omega$ model over the $\gamma - Re_\theta$ model is that it requires only one additional transport equation. On the downside, it presents two main disadvantages: (i) it is combined with the standard $k - \omega$ model and, as a consequence, inherits the freestream dependency in the fully turbulent regime and (ii) it is also not easily fine-tuned and adjusted to other underlying turbulence models or additional physics [8].

3. Simulation setup

In the study, two propellers are considered. The first one is the NACA 4-(5)(05)-041 which, despite the low freestream velocity selected for the analysis, operates at relatively high Reynolds numbers. As a consequence, the configuration with a blade torsion of $\beta_{0.75} = 20°$ is chosen for the study. Experimental data for this propeller, along with its geometric description, are available in [12]. Experimental tests were conducted on NASA's Ames 12-foot pressure wind tunnel. A default value of turbulence intensity of 0.08% was defined, as it is not specified in [12].
The second propeller is the TUD-XPROP-S [13], which operates at low Reynolds numbers due to its small diameter. For the aerodynamic study, a configuration with a blade torsion of $\beta_{0.70} = 30°$ is selected. This setting was preferred over larger pitch angles since the maximum efficiency is obtained at a high thrust setting [14]. Experimental tests were carried out at the low-speed, low-turbulence wind tunnel of the Delft University of Technology, which has turbulence intensity levels below 0.04% [15].
Table 1 compares the main geometric characteristics of both propellers, as well as their operating conditions. Additionally, in Figure 1 blade torsion and chord-to-diameter distributions along blade span for both propellers is presented.

Table 1 – Comparison of geometric characteristics and selected operating conditions for both high (NACA 4-(5)(05)-041) and low (TUD-XPROP-S) Reynolds number propellers.

(a) Propeller geometric characteristics.

Parameter	NACA 4-(5)(05)-041	TUD-XPROP-S
N	4	6
D [m]	1.22	0.2032
Airfoil	`NACA 16015`	`Clark Y`
β_{ref} [°]	20	30
$c_{0.75}/D$	0.089	0.076
$(t/c)_{0.75}$	0.047	0.061

(b) Propeller operating conditions.

Parameter	NACA 4-(5)(05)-041	TUD-XPROP-S
u_∞ [m s^{-1}]	34	30
n [rev s^{-1}]	$30.33 - 53.33$	$110.8 - 184.6$
$Re_{0.75}$	$[6.9 - 12] \cdot 10^5$	$[6.3 - 9.6] \cdot 10^4$
J	$0.920 - 0.523$	$1.332 - 0.800$
M_∞	0.1	0.087
M_{tip}	$0.36 - 0.61$	$0.22 - 0.35$

For the CFD modeling, the commercial solver `ANSYS Fluent 2025R1` is employed. The flow around the propeller is simulated using a MRF (Multiple Reference Frame) approach. The control volume is defined as a cylindrical sector around one blade due to the symmetry of the problem. The dimensions of the control volume are defined in terms of the propeller radius: the cylinder has an

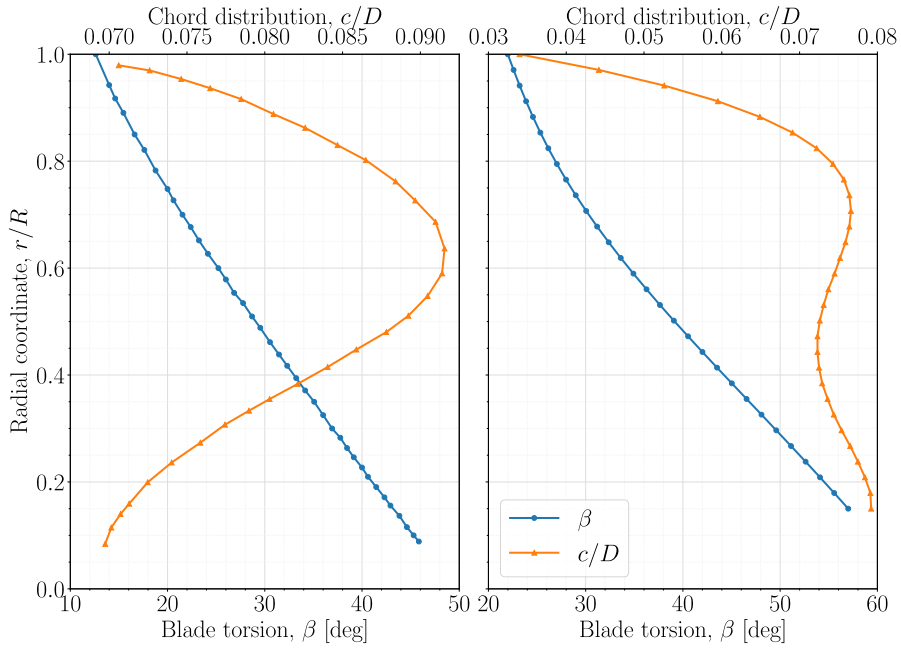


Figure 1 – Blade torsion and chord distribution for the NACA 4-(5)(05)-041 (left) [12] and TUD-XPROP-S (right) [14] propellers.

axial length of $7.5R$ (with $3R$ upstream the propeller plane) and a radius of $5.75R$ in a similar manner to that indicated in [16].

Regarding the mesh, an unstructured poly-hexcore mesh with a prism layer in the near-wall region is selected. A mesh convergence study was conducted following the index refinement concept proposed in [17, 18]. Five different grids were used, where grid 1 is the finest configuration, with h_i representing the average cell volume of the grid i. To evaluate mesh convergence, both the thrust, $C_T = T/(\rho_\infty n^2 D^4)$, and power coefficients, $C_P = P/(\rho_\infty n^3 D^5)$, were evaluated for the geometries. The number of cells, N_{cells}, and the number of divisions of the upper surface for the reference airfoil of the blade, N_{divs}, for the evaluated meshes are presented in Table 2 together with the results of the analysis, showing that convergence was achieved.

Table 2 – Mesh convergence study.

Grid	NACA 4-(5)(05)-041					TUD-XPROP-S				
	N_{cells}	h_i/h_1	N_{divs}	C_T	C_P	N_{cells}	h_i/h_1	N_{divs}	C_T	C_P
5	$3.53 \cdot 10^6$	1.587	36	0.083	0.082	$3.06 \cdot 10^6$	1.817	31	0.163	0.224
4	$5.90 \cdot 10^6$	1.357	72	0.079	0.075	$4.55 \cdot 10^6$	1.582	60	0.162	0.222
3	$9.42 \cdot 10^6$	1.161	109	0.080	0.075	$7.21 \cdot 10^6$	1.361	103	0.163	0.225
2	$11.6 \cdot 10^6$	1.082	121	0.079	0.074	$8.75 \cdot 10^6$	1.277	124	0.165	0.226
1	$14.7 \cdot 10^6$	1.000	136	0.079	0.074	$17.7 \cdot 10^6$	1.000	154	0.164	0.226

Finally, a coupled solver was employed along with the energy equation and the equation of state for ideal gasses —to account for compressibility effects—, with least-square cell for gradient terms and second order discretization schemes for the momentum, energy and turbulence closure equations. Velocity inlet boundary conditions are imposed at the inlet and on the upper cylindrical faces, while pressure outlet condition is applied at the outlet. Periodic boundary conditions are applied on the lateral faces of the cylinder and no-slip wall conditions are imposed on the propeller and hub surfaces. At the inlet, turbulence intensity is prescribed to match the experimental values, the length scale is estimated as $0.07c_{0.75}$, and, when required, intermittency is set to one [6] and laminar kinetic energy is set to zero [11].

4. Results

This section presents a discussion on the prediction of propeller performance parameters —namely, the thrust coefficient, the power coefficient and the propulsive efficiency $\eta_P = J \cdot C_T/C_P$— for several advance ratios $J = u_\infty/(nD)$, and for the different turbulence models considered in the study. Figure 2 compares the predicted performance parameters of both high and low Reynolds number propellers obtained using these turbulence models.

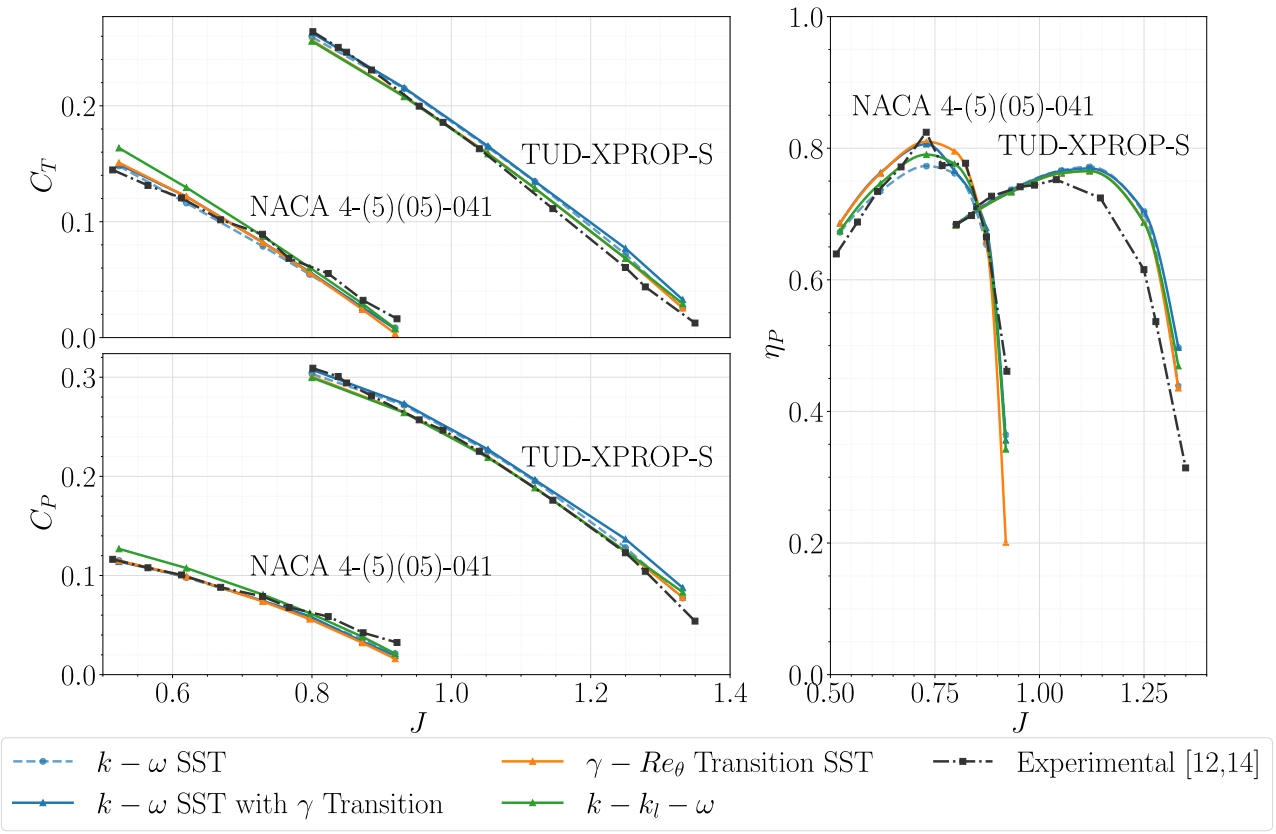


Figure 2 – Comparison of performance parameters of both high (NACA 4-(5)(05)-041) and low (TUD-XPROP-S) Reynolds number propellers for different advance ratios.

For the NACA propeller, the $k-k_l-\omega$ transition model behaves notably differently from the other models for advance ratios lower than the on-design point ($J = 0.73$). This advance ratios correspond to higher rotational speeds and therefore higher Reynolds numbers. It is worth noting how the different transition–turbulence models behave under fully turbulent flow conditions. On the one hand, intermittency-based transition models are coupled with the $k-\omega$ turbulence model. In these models, the production and destruction terms of the turbulent kinetic energy equation are modified through the intermittency factor to account for transition effects. Under fully turbulent conditions, the intermittency reaches a value of one and, as a consequence, the transition model reduces to the k–ω SST model. On the other hand, in the $k-k_l-\omega$ transition model, the laminar kinetic energy remains at low levels, with its peak value asymptotically decaying to approximately 17% of the peak turbulent kinetic energy [11]. As a result, the terms associated with bypass and natural transition become negligible, and the production of turbulent kinetic energy is no longer damped by the empirical intermittency function. Consequently, under fully turbulent conditions, the model behaviour approaches that of the standard $k-\omega$ turbulence model. This fact leads to the aforementioned discrepancies at high Reynolds numbers operating conditions of the $k-k_l-\omega$ model with the rest of the turbulent-transition models considered in this study.

In addition, all turbulence models tend to underpredict propeller performance at high advance ratios. However, propeller efficiency does not appear to be significantly affected, as it is proportional to the C_T/C_P ratio, which leads to a closer agreement with the experimental data.

On the other hand, for the TUD propeller, all turbulence models tend to overestimate propeller per-

formance at high advance ratios. As a consequence, propulsive efficiency is also overestimated for advance ratios beyond the design point. This leads to a higher propulsive efficiency and, consequently, to a predicted design point that occurs at a higher advance ratio. Note that these operating conditions correspond to lower rotational speeds and negative angles of attack on certain blade sections. Furthermore, the $k-\omega$ SST and γ transition models tend to overpredict thrust and power coefficients when compared to the $\gamma - Re_\theta$ and the $k-k_l-\omega$ transition models for all advance ratios. For clarity, Table 3 shows the relative mean square error (RMSE) computed for both C_T and C_P in order to assess the accuracy of the computations. It should be noted that experimental data for NACA 4-(5)(05)-041 exhibits two operating points at which performance coefficients appear to be overestimated, considering the overall trend of the their value across the studied range of advance ratios. This fact is clearly observable in the η_P curve shown in Figure 2.

Table 3 – Relative mean square error in the prediction of propeller performance parameters.

Turbulence model	**NACA 4-(5)(05)-041**		**TUD-XPROP-S**	
	C_T	C_P	C_T	C_P
$k-\omega$ SST *low-Re*	0.070	0.071	0.045	0.035
$\gamma - Re_\theta$ SST	0.084	0.097	0.0334	0.028
γ SST	0.0693	0.080	0.065	0.056
$k-k_l-\omega$	0.121	0.099	0.039	0.038

From the data in Table 3, it can be observed that for the high Reynolds number propeller, the use of a transition-turbulence model does not provide a clear advantage over the $k-\omega$ SST model. On the other hand, for the low Reynolds number propeller, the use of transition-turbulence models leads to improved predictions of the propeller performance parameters. For this configuration, the γ SST transition model yields the least accurate results among the models considered.

Moreover, in Figure 3 and Figure 4 the predicted distributions by transition-turbulence models of sectional thrust coefficient, $c_t = T'/(\rho_\infty n^2 D^3)$, and sectional power coefficient, $c_p = P'/(\rho_\infty n^3 D^4)$[1], are represented along blade span for on-design operating conditions for both NACA 4-(5)(05)-041 and TUD-XPROP-S propellers, respectively. Additionally, Reynolds number distribution along blade span is presented to give a deeper insight on the range of Reynolds number at which blade elements operate. The sectional Reynolds number is defined as follows:

$$Re(\hat{r}) = \frac{u_\infty c(\hat{r})}{\nu_\infty}\left[1+\left(\frac{\pi\hat{r}}{J}\right)^2\right]^{1/2}, \tag{1}$$

where $\hat{r} = r/R$ is the adimensional position along blade span.

Finally, to evaluate the efficiency of the different models for accurately assessing propeller performance, some results[2] are summarized in Table 4. To quantify the computational cost associated with each transition-turbulence model, two parameters are employed to assess the efficiency of each model:

- The average wall-clock time per iteration, τ, representing the time required by the model to compute a single iteration.
- The ratio between the number of iterations and the achieved continuity residual[3], representing the number of iterations per *unit of convergence*. It is defined as follows:

$$\eta = -\frac{N_{\text{iter}}}{\log_{10}(R_f)}. \tag{2}$$

  Note that the higher its value, the higher the number of iterations the model requires to achieve convergence.

[1] Note that T' and P' are the sectional thrust and power, respectively.

[2] Note that the simulations were performed on a computer with 128 GB DDR5 RAM memory and an `Intel Core i7-14000KF` processor (using 12 cores).

[3] The continuity residual is selected because it is the slowest to converge.

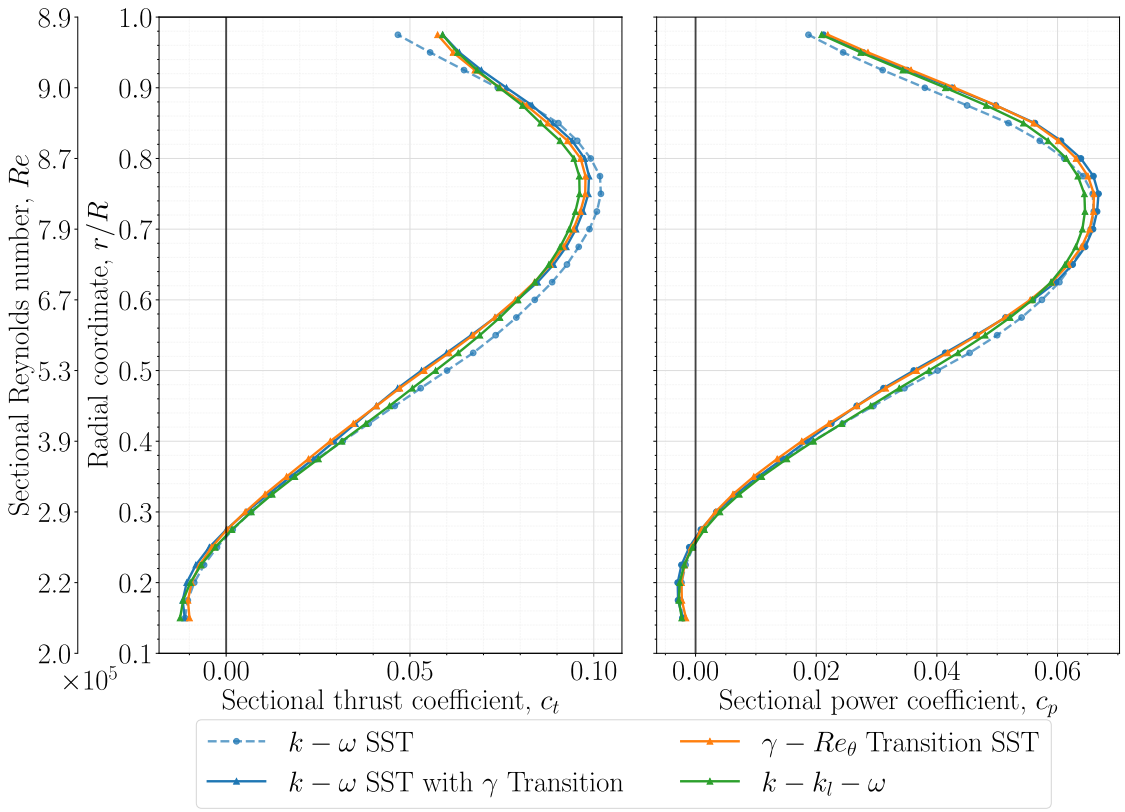


Figure 3 – Comparison of c_t and c_p distributions along blade span for on-design operating condition ($J = 0.730$) for NACA 4-(5)(05)-041 propeller.

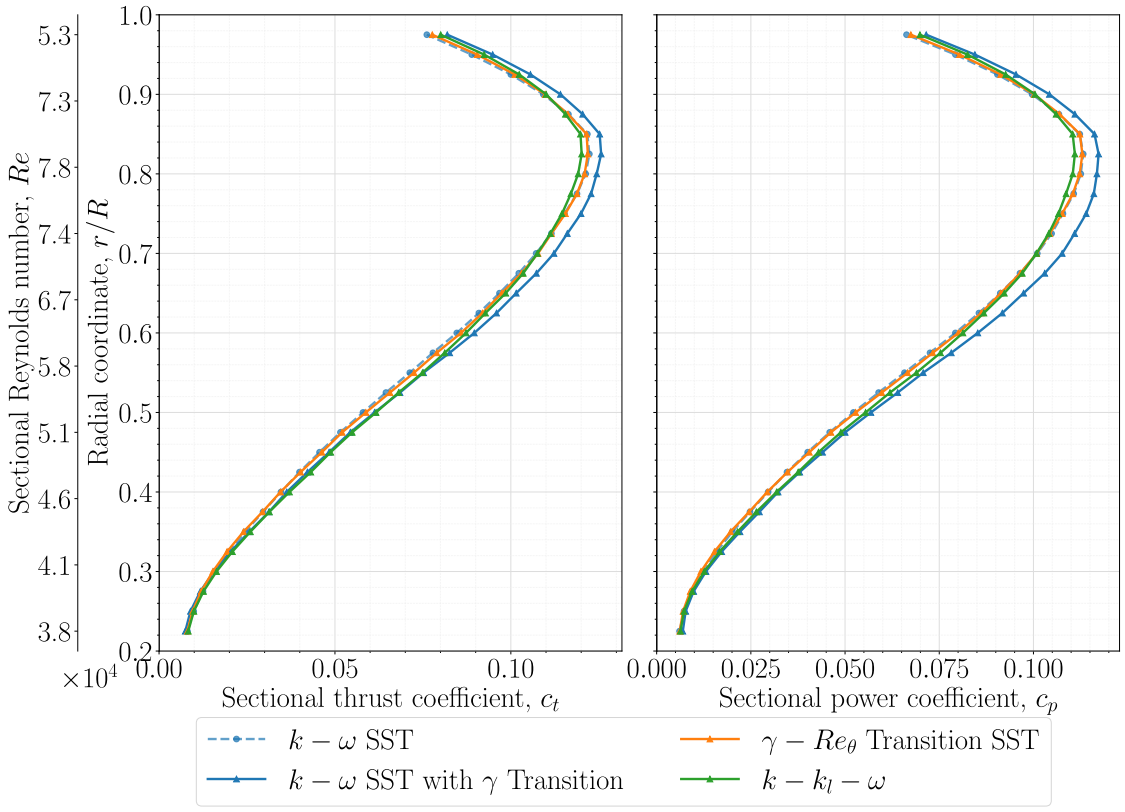


Figure 4 – Comparison of c_t and c_p distributions along blade span for on-design operating condition ($J = 1.053$) for TUD-XPROP-S propeller.

The simulation cost is computed in terms of the previous parameters as $\chi = \tau \cdot \eta$, representing the time required by each model to achieve convergence. Note that all quantities are normalized with respect to the least computationally expensive turbulence model ($k-\omega$ SST low-Re model).

Table 4 – Comparison of average wall-clock time per iteration (τ), number of iterations to achieve convergence (η) and computational cost (χ) for different turbulence models relative to the $k-\omega$ SST low-Re model.

Turbulence model	**Relative τ**	**Relative η**	**Relative χ**
$k-\omega$ SST *low-Re*	1.000	1.000	1.000
γ SST	1.076	3.244	3.491
$\gamma - Re_\theta$ SST	1.200	9.398	11.28
$k-k_l-\omega$	1.164	16.60	19.32

We have observed that the average wall-clock time per iteration for the γ transition model is approximately a 10% lower than that of the $\gamma - Re_\theta$ and $k-k_l-\omega$ transition models. Moreover, the latter two transition models exhibit a similar average wall-clock time per iteration. Additionally, the computational time for the $\gamma - Re_\theta$ transition-turbulence model is a 20% higher compared with $k-\omega$ SST which is consistent with the findings reported in [6], where an overall increase in computational time of about 20% is expected. On the other hand, regarding the number of iterations needed for each model it is observed that the higher the model complexity, the more iterations are needed to achieve the same level of convergence. It should be noted that $k-k_l-\omega$ presents a value of η approximately a 77% higher than that of the $\gamma - Re_\theta$ model denoting that it presents a slower convergence rate. This fact makes this model the one with the highest computational cost among the ones considered in this study. This agrees with the results provided in [19] where the $k-k_l-\omega$ transition model is the most time consuming to obtain a converged solution.
In summary, in Table 5 an assessment of accuracy and efficiency for the transition-turbulence models considered is shown. Accuracy is quantified as the relative mean square error in the prediction of the propeller performance parameters shown in Table 3, for each model. Its overall value is selected as $\varepsilon_{\text{RMSE}} = \max(\varepsilon_{C_T}, \varepsilon_{C_P})$. Note that the lower the value the higher the accuracy. Moreover, overall efficiency is selected as the relative computational cost, χ, shown in Table 4.

Table 5 – Summary of the accuracy and efficiency of the evaluated transition-turbulence models in predicting high and low Reynolds number propeller performance.

Turbulence model	**Accuracy**		**Efficiency**
	High Re Prop.	Low Re Prop.	
$k-\omega$ SST *low-Re*	0.071	0.045	1.000
γ SST	0.080	0.065	3.491
$\gamma - Re_\theta$ SST	0.097	0.034	11.28
$k-k_l-\omega$	0.121	0.039	19.32

5. Conclusions

This study investigated the accuracy and efficiency of transition-turbulence models in predicting propeller performance parameters. To do so, two propeller geometries operating at relatively high and low Reynolds number conditions are considered.
The results indicate that, for the high Reynolds number propeller, the use of transition–turbulence models provides no advantage over the k–ω SST turbulence model. In contrast, for the low Reynolds number propeller, the more complex models (i.e., the γ–Re_θ SST and k–k_l–ω transition–turbulence models) yield the highest accuracy, although they also incur the greatest computational cost. However, in the low Reynolds number regime, where a non-negligible portion of the flow remains laminar and the formation of laminar separation bubbles is likely, the use of these models is advisable to

accurately predict not only performance parameters, but also separation and transition-related phenomena. Among them, the γ–Re_θ SST transition–turbulence model is preferred because of its lower computational cost and the absence of the aforementioned shortcomings of the k–k_l–ω transition model, namely its sensitivity to freestream conditions and the difficulty of tuning or extending it to account for additional physics. Under relatively high Reynolds number operating conditions, where transition-related phenomena remain of interest, the γ SST model represents the best compromise between accuracy and computational efficiency.

Funding

This research was funded by Grant `PID2023-152745OA-I00`, funded by MICIU/AEI/10.13039/5011-00011033 and by ERDF/EU.

Contact Author Email Adress

Fernando Parra: fparv@unileon.es

Copyright Statement

The authors confirm that they, and/or their company or organization, hold copyright on all of the original material included in this paper. The authors also confirm that they have obtained permission, from the copyright holder of any third party material included in this paper, to publish it as part of their paper. The authors confirm that they give permission, or have obtained permission from the copyright holder of this paper, for the publication and distribution of this paper as part of the ICAS proceedings or as individual off-prints from the proceedings.

References

[1] Justin Winslow, Hikaru Otsuka, Bharath Govindarajan, and Inderjit Chopra. Basic understanding of airfoil characteristics at low reynolds numbers. *Journal of Aircraft*, 55(3):1050–1061, 2018.

[2] Jolan Wauters and Joris Degroote. On the study of transitional low-reynolds number flows over airfoils operating at high angles of attack and their prediction using transitional turbulence models. *Progress in Aerospace Sciences*, 103:52–68, 2018.

[3] Masayuki Anyoji, Taku Nonomura, Hikaru Aono, Akira Oyama, Kozo Fujii, Hiroki Nagai, and Keisuke Asai. Computational and experimental analysis of a high-performance airfoil under low-reynolds-number flow condition. *Journal of Aircraft*, 51(6):1864–1872, 2014.

[4] David C. Wilcox. Simulation of transition with a two-equation turbulence model. *AIAA Journal*, 32(2):247–255, 1994.

[5] Christopher L. Rumsey and Philippe R. Spalart. Turbulence model behavior in low reynolds number regions of aerodynamic flowfields. *AIAA Journal*, 47(4):982–993, 2009.

[6] F. R. Menter, R. B. Langtry, S. R. Likki, Y. B. Suzen, P. G. Huang, and S. Völker. A correlation-based transition model using local variables—part i: Model formulation. *Journal of Turbomachinery*, pages 413–422, 03 2004.

[7] R. B. Langtry, F. R. Menter, S. R. Likki, Y. B. Suzen, P. G. Huang, and S. Völker. A correlation-based transition model using local variables—part ii: Test cases and industrial applications. *Journal of Turbomachinery*, pages 423–434, 03 2004.

[8] Florian R. Menter, Pavel E. Smirnov, Tao Liu, and Ravikanth Avancha. A one-equation local correlation-based transition model. *Flow, Turbulence and Combustion*, 95(4):583–619, 2015.

[9] Y. B. Suzen, G. Xiong, and P. G. Huang. Predictions of transitional flows in low-pressure turbines using intermittency transport equation. *AIAA Journal*, 40(2):254–266, 2002.

[10] F. R. Menter. Two-equation eddy-viscosity turbulence models for engineering applications. *AIAA Journal*, 32(8):1598–1605, 1994.

[11] D Keith Walters and Davor Cokljat. A three-equation eddy-viscosity model for reynolds-averaged navier–stokes simulations of transitional flow. 2008.

[12] Robert M Reynolds, Robert I Samonds, and John H Walker. An investigation of single-and dual-rotation propellers at positive and negative thrust, and in combination with an naca 1-series d-type cowling at mach numbers up to 0.84. Technical report, NACA, 1957.

[13] Nando van Arnhem, Reynard de Vries, Tomas Sinnige, Roelof Vos, Georg Eitelberg, and Leo L. M. Veldhuis. Engineering method to estimate the blade loading of propellers in nonuniform flow. *AIAA Journal*, 58(12):5332–5346, 2020.

[14] Reynard de Vries, Nando van Arnhem, Tomas Sinnige, Roelof Vos, and Leo L.M. Veldhuis. Aerodynamic interaction between propellers of a distributed-propulsion system in forward flight. *Aerospace Science and Technology*, 118:107009, 2021.

[15] Delft University of Technology. Low-turbulence tunnel. https://www.tudelft.nl/lr/organisatie/afdelingen/flow-physics-and-technology/flight-performance-propulsion/flight-performance/propeller-aerodynamics/facilities/wind-tunnels, 2026.

[16] Nikolaos Mourousias, Adrián García-Gutiérrez, Ahmed Malim, Diego Domínguez Fernández, Benoît G. Marinus, and Mark C. Runacres. Uncertainty quantification study of the aerodynamic performance of high-altitude propellers. *Aerospace Science and Technology*, 133:108108, 2023.

[17] P. J. Roache. Quantification of uncertainty in computational fluid dynamics. *Annual Review of Fluid Mechanics*, 29(Volume 29, 1997):123–160, 1997.

[18] M. Hoekstra. Discretization uncertainty estimation based on a least squares version of the grid convergence index. 2006.

[19] S. M. A. Aftab, A. S. Mohd Rafie, N. A. Razak, and K. A. Ahmad. Turbulence model selection for low reynolds number flows. *PLOS ONE*, 11(4), 04 2016.